ORIGINAL RESEARCH

CURRENT DEVELOPMENTS IN NUTRITION

Vitamins and Minerals

Natural and Synthetic α-Tocopherol Modulate the Neuroinflammatory Response in the Spinal Cord of Adult *Ttpa*-null Mice

Katherine M Ranard,[1] Matthew J Kuchan,[2] Janice M Juraska,[3] and John W Erdman, Jr[1,4]

[1]Division of Nutritional Sciences, University of Illinois at Urbana-Champaign, Champaign, IL, USA; [2]Abbott Nutrition, Columbus, OH, USA; [3]Department of Psychology, University of Illinois at Urbana-Champaign, Champaign, IL, USA; and [4]Department of Food Science and Human Nutrition, University of Illinois at Urbana-Champaign, Champaign, IL, USA

ABSTRACT

Background: Vitamin E (α-tocopherol, α-T) deficiency causes neurological pathologies. α-T supplementation improves outcomes, but the relative bioactivities of dietary natural and synthetic α-T in neural tissues are unknown.

Objective: The aim was to assess the effects of dietary α-T source and dose on oxidative stress and myelination in adult α-tocopherol transfer protein–null (*Ttpa*$^{-/-}$) mouse cerebellum and spinal cord.

Methods: Three-week-old male *Ttpa*$^{-/-}$ mice ($n = 56$) were fed 1 of 4 AIN-93G–based diets for 37 wk: vitamin E–deficient (VED; below α-T limit of detection); natural α-T, 600 mg/kg diet (NAT); synthetic α-T, 816 mg/kg diet (SYN); or high synthetic α-T, 1200 mg/kg diet (HSYN). Male *Ttpa*$^{+/+}$ littermates ($n = 14$) fed AIN-93G (75 mg synthetic α-T/kg diet; CON) served as controls. At 40 wk of age, total and stereoisomer α-T concentrations and oxidative stress markers were determined ($n = 7$/group). Cerebellar Purkinje neuron morphology and white matter areas in cerebellum and spinal cord were assessed in a second subset of animals ($n = 7$/group).

Results: Cerebral cortex α-T concentrations were undetectable in *Ttpa*$^{-/-}$ mice fed the VED diet. α-T concentrations were increased in NAT (4.6 $\pm$ 0.3 nmol/g), SYN (8.0 $\pm$ 0.7 nmol/g), and HSYN (8.5 $\pm$ 0.3 nmol/g) mice, but were significantly lower than in *Ttpa*$^{+/+}$ mice fed CON (27.8 $\pm$ 1.9 nmol/g) ($P < 0.001$). *2R* stereoisomers constituted the majority of α-T in brains of *Ttpa*$^{+/+}$ mice (91%) and *Ttpa*$^{-/-}$ mice fed NAT (100%), but were substantially lower in the SYN and HSYN groups (~53%). Neuroinflammatory genes were increased in the spinal cord, but not cerebellum, of VED-fed animals; NAT, SYN, and HSYN normalized their expression. Cerebellar Purkinje neuron atrophy and myelin pathologies were not visible in *Ttpa*$^{-/-}$ mice.

Conclusions: Natural and synthetic α-T supplementation normalized neuroinflammatory markers in neural tissues of 10-mo-old *Ttpa*$^{-/-}$ mice. α-T prevents tissue-specific molecular abnormalities, which may prevent severe morphological changes during late adulthood. *Curr Dev Nutr* 2021;5:nzab008.

Keywords: vitamin E, RRR-α-tocopherol, all-*rac*-α-tocopherol, central nervous system, oxidative stress, *Ttpa*-null mouse

Manuscript received January 27, 2021. Initial review completed February 3, 2021. Revision accepted February 4, 2021. Published online February 12, 2021.
This work was supported by Abbott Nutrition through the Center for Nutrition, Learning, and Memory (CNLM) at the University of Illinois, a USDA Hatch grant (ILLU-698-915), and the Division of Nutritional Sciences Margin of Excellence Research Program at the University of Illinois. KMR was supported by the Agriculture and Food Research Initiative (AFRI) National Institute of Food and Agriculture (NIFA) Predoctoral Fellowships Grant Program (2019-67011-29514) from the USDA, NIFA.

Author disclosures: MJK is employed by Abbott Nutrition, which supported this work. Beyond the disclosure of MJK, Abbott Nutrition had no role in the study design, implementation, analysis, or interpretation of the data. The other authors report no conflicts of interest.

Address correspondence to JWE (e-mail: jwerdman@illinois.edu).

Supplemental Figures 1–6 and Supplemental Tables 1–3 are available from the "Supplementary data" link in the online posting of the article and from the same link in the online table of contents at https://academic.oup.com/cdn/.

Abbreviations used: all-*rac*, all-*racemic*; AVED, ataxia with vitamin E deficiency; *Ccl2*, chemokine (C-C motif) ligand 2; CON, control; HSYN, high synthetic α-tocopherol; *Il1b*, interleukin 1B; LXR, liver X receptor; NAT, natural α-tocopherol; *Necab1*, neuronal calcium binding protein1; PDA, photodiode array detection; SYN, synthetic α-tocopherol; *Ttpa*, α-tocopherol transfer protein; VED, vitamin E–deficient; 3-NT, 3-nitrotyrosine; 4-HNE, 4-hydroxynonenal; α-T, α-tocopherol; α-TA, α-tocopheryl acetate; α-TTP, α-tocopherol transfer protein.

Introduction

Oxidative stress is associated with many neurological diseases (1). Vitamin E [α-tocopherol (α-T)] is an essential lipid-soluble antioxidant that protects membrane lipids, including the highly abundant and peroxidation-prone PUFAs in the brain and spinal cord (2, 3). Accordingly, α-T deficiency promotes lipid peroxidation and causes neurological and neuromuscular disorders in humans and animal models (4, 5). Familial ataxia with vitamin E deficiency (AVED) is a human condition caused by loss-of-function mutations in the gene encoding α-T transfer protein (α-TTP). In the liver, α-TTP regulates the intracellular trafficking of α-T and facilitates α-T export into circulating lipoproteins (6).

The α-tocopherol transfer protein–null (*Ttpa*$^{-/-}$) mouse model, generated by deleting the translational start codon of the α-TTP gene

(7), recapitulates AVED symptoms. The timeline of the disease appears to differ between AVED patients and *Ttpa*$^{-/-}$ mice; humans typically manifest severe clinical signs during childhood (8), whereas *Ttpa*$^{-/-}$ mice do not exhibit severe abnormalities until adulthood (9–11). Molecular changes, such as increased oxidative stress and neuroinflammatory stress, may occur earlier in *Ttpa*$^{-/-}$ mice, before measurable structural or behavioral changes. However, our knowledge of the developmental timeline is incomplete. Most *Ttpa*$^{-/-}$ mouse studies focus on the effects of α-T status during aging. At what age are specific tissues or cell types affected, and which alterations happen first?

Our analyses targeted the cerebellum and spinal cord, 2 tissues implicated in α-T deficiency symptomology. Specifically, in the cerebellum, Purkinje neuron injury may exacerbate the ataxic phenotype observed in AVED patients (12). Purkinje neurons are key mediators of motor output, and their function is essential for balance and coordination (13, 14). Aging adult (17-mo-old) *Ttpa*$^{-/-}$ mice have Purkinje neuron atrophy, with reduced dendritic branching and smaller cell bodies (10). Oxidative stress markers, such as 3-nitrotyrosine (3-NT) and thiobarbituric acid reactive substances (TBARS), are also elevated in cerebella of 17- and 20-mo-old *Ttpa*$^{-/-}$ mice, respectively (10, 11). However, Purkinje neuron morphology and cerebellar oxidative stress markers have not been thoroughly evaluated in *Ttpa*$^{-/-}$ mice at earlier ages.

In the spinal cord, the transcriptomic profiles of 6-mo-old *Ttpa*$^{-/-}$ mice suggested the dysregulation of inflammation and innate immune response pathways (9). The expression of the transcription factor liver X receptor (LXR) and its gene targets were also upregulated by age in adult *Ttpa*$^{-/-}$ mice (9). LXR regulates multiple processes, such as cholesterol metabolism, inflammatory signaling, and myelination (15). Myelin is a lipid-rich insulator that wraps around axons and optimizes the nerve signal conduction speed. Myelin defects have been observed in the dorsal spinal column of adult *Ttpa*$^{-/-}$ mice, evidenced by a reduced number of myelinated fibers (11) and loosely organized myelin sheaths (9).

In sum, these studies have established the profound influence of low α-T status on immune response and myelination in neurological tissues, which culminates in neurobehavioral manifestations. Importantly, α-T supplementation reduces α-T deficiency symptoms in both AVED patients and *Ttpa*$^{-/-}$ mice (10, 11, 16–18). However, the source of α-T supplementation should be considered, as humans consume both naturally occurring (*RRR*) α-T from plant components like seed oils and synthetic [all-*racemic* (all-*rac*), a mixture of stereoisomers including *RRR*] α-T from α-T–fortified food products and supplements. The natural α-T stereoisomer is preferentially retained by hepatic α-TTP (19), and consequently accumulates in neurological tissues more than the synthetic α-T stereoisomers (20–22). Natural α-T is also more biopotent than synthetic α-T (23), but their relative potencies in the central nervous system are unknown (24).

Few studies have directly compared the neurological effects of synthetic α-T versus natural α-T using murine models. In our previous study using adolescent *Ttpa*$^{-/-}$ mice, dietary synthetic α-T downregulated myelination-related genes in the cerebellum compared with natural α-T (25). These findings suggested that α-T sources differentially affect brains of young mice. Other mouse studies have similarly demonstrated that α-T sources differentially modulate the transcriptomes of the hippocampus (22) and T-lymphocytes (26).

The goal of our current study was to compare natural versus synthetic α-T during adulthood, when neurological tissues are more susceptible to oxidative stress and associated neurological deficits. We chose to evaluate animals when they were 10 mo old; this age represents an intermediary stage of adulthood and helps fill the gap between our previous adolescent mouse study (~2 mo old) and the aging adult mouse studies (~17–20 mo old). As in our adolescent *Ttpa*$^{-/-}$ mouse study, diets were supplemented with either natural α-T or 1 of 2 doses of synthetic α-T. The synthetic α-T diet levels were 1.36 times and 2 times the levels by mass of the natural α-T diet. These concentrations reflect the 2 hypothesized ratios of biopotency (1.36:1 and 2:1) for natural versus synthetic α-T, which were proposed based on rat fetal-resorption assays and the affinity of α-TTP to the *2R* and *2S* stereoisomers, respectively (23, 27).

We used a combination of transcriptomic, biochemical, and histological approaches to comprehensively characterize the 10-mo-old adult *Ttpa*$^{-/-}$ mouse cerebellum and spinal cord. Our primary finding was that *Ttpa*$^{-/-}$ mice fed a vitamin E–deficient (VED) diet had upregulated expression of neuroinflammatory genes (e.g., the cytokine *Tnf*) in the spinal cord but not cerebellum. Furthermore, both natural and synthetic α-T normalized their expression. Our work contributes to the developmental timeline of α-T deficiency hallmarks, reinforces the benefits of dietary α-T, and provides a foundation for future studies evaluating natural versus synthetic α-T in neural tissues.

Methods

Animals

The University of Illinois Institutional Animal Care and Use Committee approved all animal procedures. *Ttpa*$^{-/-}$ males were crossed with C57BL/6 (*Ttpa*$^{+/+}$) females to produce heterozygous *Ttpa*$^{+/-}$ mice. Female *Ttpa*$^{+/-}$ offspring were fed a previously described AIN-93G–based low-vitamin-E diet [35 mg all-*rac*–α-tocopheryl acetate (-α-TA)/kg diet] (28). These *Ttpa*$^{+/-}$ mice were then bred to generate *Ttpa*$^{+/+}$ and *Ttpa*$^{-/-}$ offspring to be used for the current study. The low-vitamin-E breeder diet minimized brain α-T concentrations in the *Ttpa*$^{-/-}$ mice weanlings (3.38 $\pm$ 0.64 nmol/g), similar to previous reports (9, 25, 28).

Offspring were genotyped, and on postnatal day 21 male *Ttpa*$^{+/+}$ and *Ttpa*$^{-/-}$ mice were weaned onto their assigned experimental diet, exactly as described in our adolescent mouse study (25). Both the previous study and the current study used exclusively males; this aided in the comparison of findings.

Study animals were individually housed in shoebox cages (12:12-h light-dark cycle, 22°C, 60% humidity) with ad libitum access to food and water until study termination at 40 wk of age (37-wk feeding period). Body mass and food intake were measured on a weekly basis. Diet was removed from cages ~12 h before being killed. Mice were killed via different protocols, according to which analyses their tissues were preassigned.

For biochemical and gene expression analyses (n = 7/group), mice were anesthetized with isoflurane, and blood was collected via cardiac puncture. Serum was separated by centrifugation (1500 × g for 15 min, 4°C; Centrifuge 5417R, Eppendorf). Following decapitation, other tissues were dissected, weighed, and snap-frozen in liquid nitrogen. Target

brain regions (cerebral cortex and cerebellum) were further dissected. One-half of each cerebellum was placed in RNA*later*® (Thermo Fisher) before freezing. The remaining brain regions were used as a "composite" brain sample for α-T stereoisomer analysis. All tissues were stored at −80°C until analysis.

Mice used to assess cerebellar Purkinje neuron morphology and white matter areas in the cerebellum and spinal cord ($n = 7$/group) were anesthetized with isoflurane and perfused intracardially with a 0.1-M solution of PBS, followed by a 4% paraformaldehyde fixative solution in PBS (pH 7.4). Brains and cervical spinal cord segments were extracted and post-fixed in paraformaldehyde solution for 24 h, followed by a 30% sucrose solution (cryoprotectant) for 72 h. A freezing microtome was used to slice 40-μm sagittal sections of brain and 40-μm transverse sections of spinal cord. All animal tissues were coded to conceal their diet group from the experimenters. Sections were stored at −20°C in antifreeze storage solution (30% glycerol, 30% ethylene glycol, 30% distilled water, 10% 0.2 M PBS), until stained with methylene blue/Azure II.

Diets

All experimental diets (modified AIN-93G formulas) and associated procedures matched those used in our previous adolescent mouse study (25). *RRR*-α-TA (Novatol 700D; Archer Daniels Midland) and all-*rac*-α-TA (Sigma-Aldrich) were added to the natural α-T (NAT) and synthetic α-T/high synthetic α-T (SYN/HSYN) diets, respectively. Before diet preparation, both α-TA ingredients were analyzed via HPLC with photodiode array detection (HPLC-PDA) to verify α-TA concentrations (25). *Ttpa*$^{+/+}$ mice were fed a control diet (CON; 75 mg all-*rac*-α-TA/kg diet). *Ttpa*$^{-/-}$ mice were preassigned to 1 of 4 diets: VED (below α-TA limit of detection), NAT (600 mg *RRR*-α-TA/kg diet), SYN (816 mg all-*rac*-α-TA/kg diet), or HSYN (1200 mg all-*rac*-α-TA/kg diet). The α-TA concentration in the NAT diet (600 mg *RRR*-α-TA/kg diet) matched the α-TA concentration used in previous *Ttpa*$^{-/-}$ studies; this concentration was necessary to improve neurological symptoms in *Ttpa*$^{-/-}$ mice (9–11). The SYN and HSYN diets were subsequently formulated to contain 1.36 times or 2 times the α-TA by mass of the NAT diet, respectively. These relative α-TA diet levels therefore represent the 2 proposed ratios of biopotency between natural and synthetic α-T (1.36:1 and 2:1). Concentrations of α-TA in the 5 study diets were determined via HPLC-PDA, as described previously (25). The analyzed values were consistent with the planned diet formulations. Diets were stored at −20°C in vacuum-sealed packages, and new diet was provided to mice each week.

Vitamin E analysis

The extractions, data processing, and analysis of α-TA from experimental diets, as well as total α-T and brain stereoisomer profiles, were carried out using HPLC methods exactly as described previously (25). The lower limit of detection for α-T in serum and tissues was 0.11 μmol/L and 0.12 nmol/g, respectively.

Total RNA isolation and RT-qPCR analysis

Total RNA was isolated from the cerebellum and spinal cord as previously described (29). RNA purities and concentrations were determined, followed by cDNA synthesis. RT-qPCR was performed on a StepOnePlus Real-Time PCR System (Applied Biosystems) following the manufacturer's protocol for SYBR® Green ROX qPCR Mastermix (Qiagen). Relative quantitation of gene expression was calculated using the $2^{-\Delta\Delta Ct}$ method. Actin B1 (*Actb1*) was used as the housekeeping gene. Genes related to oxidative stress and myelination were selected based on findings from previous *Ttpa*$^{-/-}$ mouse studies (9, 25, 30–32) (**Table 1**). Primers were purchased from Integrated DNA Technologies, and primer sequences are listed in **Supplemental Table 1**.

TABLE 1 Selected oxidative stress– and myelination-related genes for RT-qPCR analysis in the cerebellum and spinal cord[1]

Myelination	Oxidative stress	Additional genes
Car8	*Tnf*	*Necab1*
Cnp	*Ccl2*	*Ttpa*
Mag	*Il6*	
Mbp	*Il1b*	
Mobp		
Myrf		
Plp1		
Rora		
Sox10		

[1]Select genes were only analyzed in either the cerebellum (*Rora*) or spinal cord (*Ccl2*, *Il6*, *Il1b*, *Nr1h3*). *Car8*, carbonic anhydrase 8; *Ccl2*, chemokine (C-C motif) ligand 2; *Cnp*, 2′,3′-cyclic nucleotide 3′ phosphodiesterase; *Il1b*, interleukin 1B; *Il6*, interleukin 6; *Necab1*, neuronal calcium binding protein 1; *Mag*, myelin-associated glycoprotein; *Mbp*, myelin basic protein; *Mobp*, myelin-associated oligodendrocytic basic protein; *Myrf*, myelin regulatory factor; *Plp1*, proteolipid protein (myelin) 1; *Rora*, RAR-related orphan receptor alpha; *Sox10*, sex determining region Y-box 10; *Tnf*, tumor necrosis factor; *Ttpa*, α-tocopherol transfer protein.

Lipid peroxidation

4-Hydroxynonenal (4-HNE) was analyzed in cerebellar and spinal cord extracts by ELISA (OxiSelect HNE AdductELISA Kit; Cell Biolabs) according to the manufacturer's instructions. Briefly, total protein was extracted with RIPA buffer (Thermo Scientific) containing 1% protease inhibitor cocktail (Sigma) at 4°C. Protein concentrations were determined by the Pierce BCA protein assay kit (Thermo Scientific). All samples (150 μg total protein each) were run in duplicate.

Cerebellar Purkinje neuron morphology and myelinated axon areas

Single sagittal brain sections (40 μm from the midline) and cervical spinal cord sections (C2–C3 region) were washed with a 0.1 M PBS solution and mounted on electrostatically charged slides. Once dry, slices were stained with a cell body stain (methylene blue/Azure II), and then coverslipped with Permount (Fisher Scientific).

Digital images of brain and spinal cord sections were acquired using an AxioSkop 40 Zeiss microscope equipped with an AxioCam MRc5 camera and Zen Blue software. Purkinje neuron cell body areas were measured in matched regions of cerebellar lobules III, VI, and VIII (>200 somas/mouse; $n = 7$ mice/group). The ImageJ region of interest (ROI) Manager tool (33) was used to trace around each individual soma and calculate area.

White matter areas contain myelinated axons and can be used as a gross approximation of the amount of myelination, as well as a visual marker of atrophy (34). These areas were traced in the cerebellum and spinal cord using ImageJ. Single sections of each tissue were analyzed for each mouse ($n = 7$/group).

TABLE 2 Total α-T accumulation in selected tissues of *Ttpa*$^{+/+}$ and *Ttpa*$^{-/-}$ mice fed experimental diets[1]

	Ttpa$^{+/+}$	*Ttpa*$^{-/-}$			
Tissue	CON	VED	NAT	SYN	HSYN
Serum	11.3 ± 2.0^{a}	ND[2]	2.7 ± 0.4^{b}	6.1 ± 1.1^{c}	5.4 ± 0.5^{c}
Liver	108.5 ± 22.9^{a}	ND	123.9 ± 36.6^{a}	334.6 ± 46.2^{a}	542.6 ± 77.4^{b}
Heart	32.0 ± 1.0^{a}	ND	32.3 ± 2.0^{a}	77.4 ± 5.5^{b}	95.9 ± 6.2^{b}
Lung	22.5 ± 3.3^{a}	ND	27.6 ± 3.8^{a,b}	56.4 ± 11.8^{b}	54.9 ± 6.6^{b}

[1]Values are expressed as mean ± SEM μmol/L (serum) or nmol/g (other tissues); n = 7/group. For each tissue type, different superscript letters denote significant differences ($P < 0.05$) between experimental groups by either 1-factor ANOVA with Tukey's post hoc test (serum, heart, lung) or the nonparametric Kruskal-Wallis test (liver). CON, control AIN-93G diet; HSYN, high synthetic α-tocopherol; NAT, natural α-tocopherol; ND, not detected; SYN, synthetic α-tocopherol; *Ttpa*, α-tocopherol transfer protein; VED, vitamin E–deficient; α-T, α-tocopherol.
[2]Lower limits of detection: 0.11 μmol/L (serum); 0.12 nmol/g (tissues). Three and 2 VED-fed mice had very low but detectable concentrations (<2 nmol/g) in the liver and heart, respectively.

Statistical analysis

All data were analyzed using GraphPad Prism version 8.1.3 for Windows (GraphPad Software). Normality and homogeneity of variance were evaluated using the Shapiro-Wilk and Brown-Forsythe tests, respectively. If data did not meet these assumptions, values were transformed via logarithm or square-root functions; if assumptions were still not met after transforming the data, the nonparametric Kruskal-Wallis test with Dunn's post hoc was used. Time- and treatment-dependent changes in body mass and food intake were analyzed by fitting a mixed-effects 2-factor repeated-measures ANOVA model due to missing values. Pearson's correlation test was used to test for significant correlations between variables. For most study endpoints, differences between diet groups were analyzed by 1-factor ANOVA, followed by Tukey's post hoc test when justified; differences between diet groups were considered significant when $P < 0.05$. For gene expression data, significance was assigned following an additional Bonferroni correction: $P < 0.003$ for spinal cord (0.05/15 genes) or $P < 0.004$ for cerebellum (0.05/12 genes).

Results

Body mass, brain mass, and food intake

Body mass increased over time for all mice ($P < 0.001$), but there were no significant differences between diet groups ($P = 0.147$) (**Supplemental Figure 1**). Brain mass did not differ between groups ($P = 0.635$; data not shown). There was a significant time effect for average weekly food intake ($P < 0.001$), but no differences between groups ($P = 0.286$) (Supplemental Figure 1).

α-T bioaccumulation in nonneurological tissues

α-T concentrations in *Ttpa*$^{-/-}$mice fed the VED diet were below the lower limit of detection for all nonneurological tissues analyzed, including serum, liver, heart, and lung (**Table 2**). NAT, SYN, and HSYN diets increased α-T concentrations to varying degrees, depending on the tissue type. SYN and HSYN diets significantly increased serum α-T concentrations compared with the NAT diet, but were still only ~50% of the α-T concentrations of *Ttpa*$^{+/+}$mice fed the CON diet. In contrast, the α-T–supplemented diets increased liver, heart, and lung α-T concentrations to equal or greater α-T concentrations than in the CON diet group (Table 2). Generally, the α-T tissue concentrations in *Ttpa*$^{-/-}$ mice increased as total α-T mass in the diet increased.

Brain α-T bioaccumulation

Cerebral cortex α-T concentrations were below the limit of detection in the VED diet group (**Figure 1**A). α-T-supplemented diets increased total α-T concentrations, with significantly higher concentrations in the SYN and HSYN groups compared with the NAT group ($P < 0.01$). NAT,

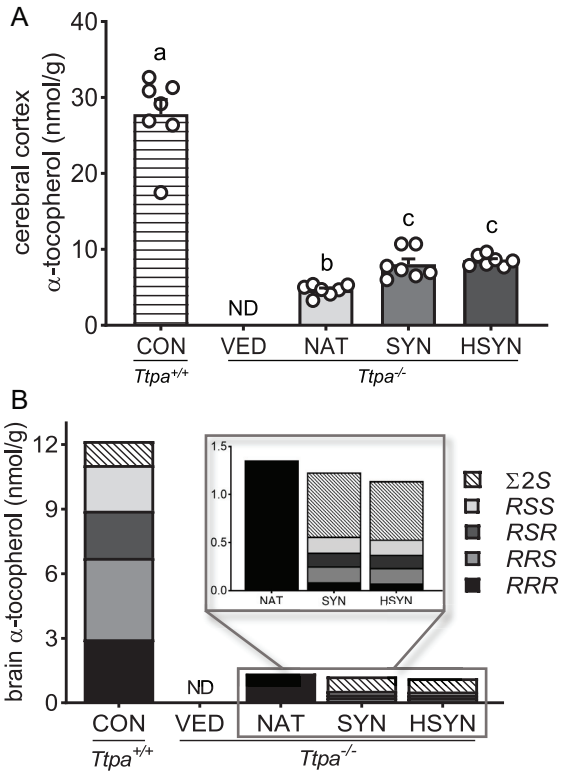

FIGURE 1 Brain α-T concentrations and stereoisomer profiles in adult *Ttpa*$^{+/+}$ and *Ttpa*$^{-/-}$ mice after 37 wk of being fed experimental diets. (A) Cerebral cortex values are expressed as means ± SEMs (n = 7/group). Each circle represents the measured value from an individual mouse. Different superscript letters denote significant differences between experimental groups ($P < 0.01$). (B) α-T stereoisomer profiles in a pooled composite brain sample from each diet group (n = 7/group). Lower limit of detection: 0.12 nmol/g. CON, control AIN-93G diet; HSYN, high synthetic α-tocopherol; NAT, natural α-tocopherol; ND, not detected; SYN, synthetic α-tocopherol; *Ttpa*, α-tocopherol transfer protein; VED, vitamin E–deficient; α-T, α-tocopherol.

SYN, and HSYN group concentrations were all significantly lower than in the CON group.

Brain α-T stereoisomer profiles were assessed using a pooled composite sample for each experimental group (Figure 1B). The majority of α-T in brains of $Ttpa^{+/+}$ mice fed the CON diet consisted of *2R* stereoisomers (91%). The most abundant stereoisomer was *RRS* (31%), followed by the naturally occurring stereoisomer *RRR* (24%), *RSR* (18%), and *RSS* (17%). *RRR*-α-T was the only detectable stereoisomer in $Ttpa^{-/-}$ mice fed the NAT diet, which is consistent with the α-T source in their diet. $Ttpa^{-/-}$ mice fed either SYN or HSYN diets had similar α-T stereoisomer profiles; their brains did not show discrimination between *2R* (∼53%) and *2S* (∼47%) stereoisomers. Interestingly, *RRR* constituted the lowest proportion of α-T (∼6%) in these mice, while the other *2R* stereoisomers constituted relatively higher proportions (∼11–14%).

Ttpa expression in cerebellum and spinal cord

The $Ttpa^{-/-}$ mouse model was generated via the insertion of *lacZ* (β-galactosidase) and *neo* (neomycin phosphotransferase) genes into the 5′ untranslated sequences of exon 1 of the α-T transfer protein gene (*Ttpa*) (7). This resulted in the deletion of the *Ttpa* translational start codon. $Ttpa^{-/-}$ mice may still express the mRNA to some degree, but these transcripts are not translated into functional proteins. In the current study, *Ttpa* was detectable in neural tissues of all mice. All $Ttpa^{-/-}$ mouse groups had significantly lower *Ttpa* expression than the $Ttpa^{+/+}$ group in both the cerebellum (∼2.7-fold lower) and spinal cord (∼6.6-fold lower) ($P < 0.001$) (**Supplemental Figure 2**). Neither dietary α-T source nor dose affected *Ttpa* expression. Notably, our study is not the first to detect *Ttpa* transcripts in neurological tissues of *Ttpa*-null mice (9).

Cerebellar oxidative stress

Tnf expression was used as a cytokine gene marker for the neuroinflammatory response; its expression did not differ between diet groups in the cerebellum (**Supplemental Table 2**). The lipid peroxidation product 4-HNE tended to be higher in the VED group (**Figure 2**A), but there was substantial biological variability between mice ($P = 0.31$). In support of the relation between oxidative stress markers in this study, 4-HNE concentrations were significantly positively correlated with *Tnf* expression ($r = 0.38$, $P = 0.026$) (Figure 2B).

Cerebellar myelination

Neuronal calcium binding protein 1 (*Necab1*) expression was significantly downregulated in all $Ttpa^{-/-}$ mouse groups, regardless of diet (∼0.2-fold change, $P < 0.001$). These results corroborate those of a previous study that also reported 0.2-fold change in cerebella of 6-mo-old $Ttpa^{-/-}$ mice (9). The selected myelination-related genes (*Car8*, carbonic anhydrase 8; *Cnp*, 2′,3′-cyclic nucleotide 3′ phosphodiesterase; *Mag*, myelin-associated glycoprotein; *Mbp*, myelin basic protein; *Mobp*, myelin-associated oligodendrocytic basic protein; *Myrf*, myelin regulatory factor; *Plp1*, proteolipid protein myelin 1; *Rora*, RAR-related orphan receptor alpha; *Sox10*, sex determining region Y-box 10) were not significantly modulated by genotype or α-T supplementation in the cerebellum (**Supplemental Figure 3**; Supplemental Table 2). There were no differences in the cerebellar white matter area between groups, which was used as an estimate of relative myelinated axon quantity (**Figure 3**A).

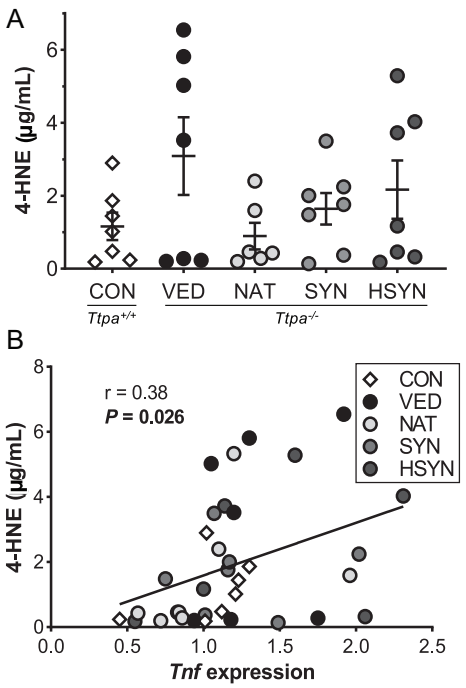

FIGURE 2 Lipid peroxidation in cerebella of adult $Ttpa^{+/+}$ and $Ttpa^{-/-}$ mice after 37 wk of being fed experimental diets. (A) 4-HNE values are expressed as means ± SEMs ($n = 5$–7/group). There were no significant differences by 1-factor ANOVA ($P = 0.31$). (B) Positive correlation between cerebellar 4-HNE concentrations and *Tnf* expression. Points represent individual mice and are color coded by diet group. Correlations were evaluated by Pearson's correlation test. CON, control AIN-93G diet; HSYN, high synthetic α-tocopherol; NAT, natural α-tocopherol; SYN, synthetic α-tocopherol; *Ttpa*, α-tocopherol transfer protein; VED, vitamin E–deficient; 4-HNE, 4-hydroxynonenal.

Cerebellar Purkinje neuron morphology

Average Purkinje neuron cell body sizes were not altered in $Ttpa^{-/-}$ mice fed the VED diet or fed α-T–supplemented diets (Figure 3C–F). Notably, we analyzed a relatively large group of mice ($n = 7$/group) compared with a previous study that only evaluated $n = 2$–3/group. Similar to our cerebellar 4-HNE results, there was substantial biological variability between mice. Purkinje neuron atrophy may not reliably occur in $Ttpa^{-/-}$ mice until they are older (∼17 mo) (10), when the cerebellum is more vulnerable to oxidative stress. Consequently, morphological benefits of supplemental α-T may not be visible until older ages.

Spinal cord oxidative stress

Tnf expression was increased in the spinal cord of $Ttpa^{-/-}$ mice fed the VED diet ($P = 0.02$) (**Figure 4**A), suggesting a neuroinflammatory response at the transcriptome level. NAT, SYN, and HSYN diets all normalized *Tnf* expression. Additional oxidative stress–related genes [chemokine (C-C motif) ligand 2 (*Ccl2*), interleukin 1B (*Il1b*), *Il6*] were analyzed to probe the neuroinflammatory hypothesis. These

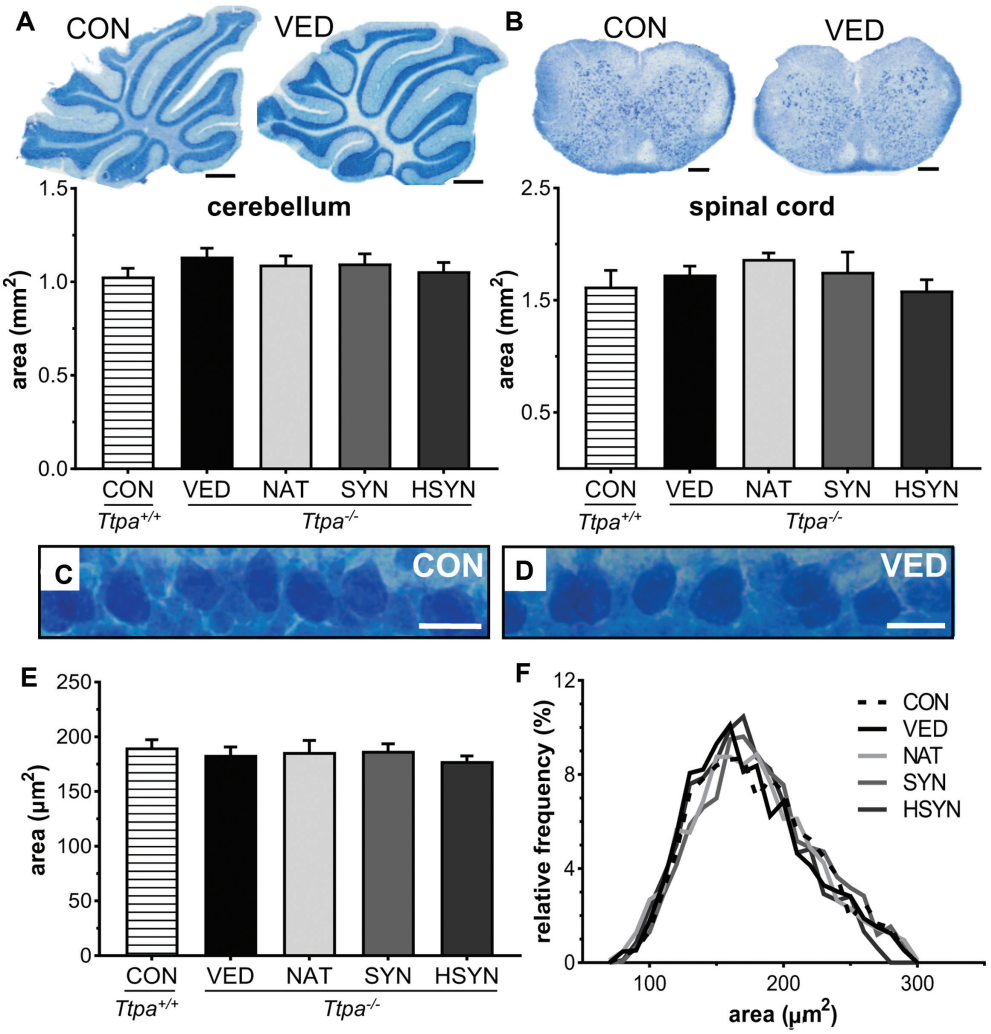

FIGURE 3 Cerebellum and spinal cord morphology in adult $Ttpa^{+/+}$ and $Ttpa^{-/-}$ mice after 37 wk of being fed experimental diets. White matter areas: (A) cerebellum, scale bar: 0.5 mm; (B) spinal cord, scale bar: 250 μm. Values are expressed as means ± SEMs ($n = 7$/group). There were no significant differences between groups by 1-factor ANOVA. (C, D) Representative Purkinje neuron layers for CON and VED diet groups, original magnification, 40×; scale bar: 20 μm. (E) Purkinje cell body areas are expressed as means ± SEMs ($n = 7$/group). (F) Frequency distribution of cell body sizes for all diet groups. There were no differences between groups for cerebellar Purkinje neuron analyses. CON, control AIN-93G diet; HSYN, high synthetic α-tocopherol; NAT, natural α-tocopherol; SYN, synthetic α-tocopherol; *Ttpa*, α-tocopherol transfer protein; VED, vitamin E–deficient.

genes are also downstream targets of the TNF signaling pathway. Both *Ccl2* ($P = 0.06$) and *Il1b* ($P = 0.03$) were nonsignificantly increased in the VED group compared with the CON group, and levels were normalized with α-T supplementation (Figure 4B). *Tnf*, *Ccl2*, and *Il1b* expression values varied substantially between mice in the VED group, but the 3 genes were consistently higher or lower for each individual mouse (**Supplemental Figure 4**). There were significant positive correlations between *Tnf* versus *Ccl2* expression ($r = 0.77$, $P < 0.001$) and *Tnf* versus *Il1b* expression ($r = 0.83$, $P < 0.001$) (**Supplemental Figure 5**). These associations align with the known relations between *Tnf* and downstream target genes, and further support the observed neuroinflammatory gene changes between diet groups.

Spinal cord lipid peroxidation, as indicated by 4-HNE concentrations, was similar across all diet groups (**Supplemental Figure 6**).

Spinal cord myelination

In the spinal cord, myelination-related genes (*Car8*, *Cnp*, *Mag*, *Mbp*, *Mobp*, *Myrf*, *Plp1*, *Nr1h3*, *Sox10*) were similarly expressed across all diet groups (Supplemental Figure 3; **Supplemental Table 3**). There were also no differences in white matter areas (Figure 3B).

Discussion

The goal of this work was to compare the effects of natural versus synthetic α-T in the cerebellum and spinal cord of $Ttpa^{-/-}$ mice. We assessed adult mice (10 mo old) to fill a gap in experimental knowledge; previous studies focused on mice at other life stages, primarily aging adulthood (~17–20 mo old). Neuroinflammatory genes were upregulated in the spinal cord of 10-mo-old $Ttpa^{-/-}$ mice fed the VED

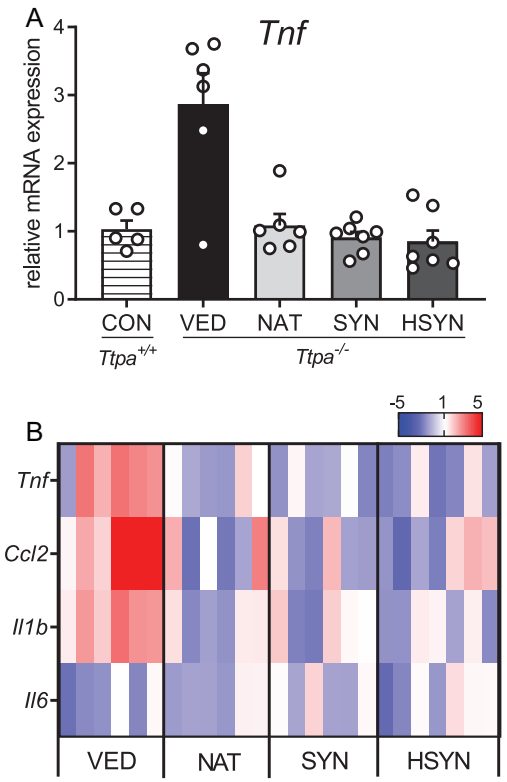

FIGURE 4 Neuroinflammatory genes in spinal cord of adult *Ttpa*$^{+/+}$ and *Ttpa*$^{-/-}$ mice after 37 wk of being fed experimental diets. (A) *Tnf* values, expressed as means ± SEMs (n = 5–7/group). (B) Additional neuroinflammatory genes were tested to confirm diet trends observed with *Tnf*. Heatmap colors indicate average fold-changes relative to the CON diet group, and each column represents an individual mouse. There were no significant differences between groups, but trends were observed for CON vs. VED comparisons: *Tnf*, $P = 0.02$; *Ccl2*, $P = 0.06$; *Il1b*, $P = 0.03$. *Ccl2*, chemokine (C-C motif) ligand 2; CON, control AIN-93G diet; HSYN, high synthetic α-tocopherol; *Il1b*, interleukin 1B; *Il6*, interleukin 6; NAT, natural α-tocopherol; SYN, synthetic α-tocopherol; *Ttpa*, α-tocopherol transfer protein; VED, vitamin E–deficient.

diet, and both natural and synthetic α-T supplementation normalized this gene expression profile. Contrary to our original hypothesis, these changes did not occur in the cerebellum. However, these tissue-specific findings align with work published after our trial began, using 6- and 12-mo-old *Ttpa*$^{-/-}$ mice (9); they proposed that the spinal cord is the initial site of α-T deficiency pathology in the *Ttpa*$^{-/-}$ mouse model. More profound cerebellar abnormalities may not occur until later in adulthood (~17 mo old) (10), or possibly during the unstudied age window of 12–17 mo old (**Figure 5**).

We measured select genes related to neuroinflammation, such as *Tnf*, rather than conducting a full transcriptome analysis. α-T status modulates *Tnf* expression in various inflammatory contexts, in both cell and animal models (35–37). The current study contributes additional in vivo evidence for this relation in the central nervous system. *Tnf* was also positively correlated with other selected TNF signaling pathway genes (*Ccl2*, *Il1b*) in the spinal cord. α-T status clearly modulates gene expression, directly or indirectly resulting in downstream consequences. In addition, our *Tnf* results may implicate TNF-producing immune cells, specifically T cells, in the response to low vitamin E status.

The lipid peroxidation product 4-HNE was nonsignificantly increased in the cerebellum of VED mice, and there were no changes in the spinal cord. A previous study reported increased 4-HNE concentrations in both the cerebellum and spinal cord of ~20-mo-old *Ttpa*$^{-/-}$ mice (11), but 10 mo of age may not be old enough to detect these changes. Tissue-specific, or possibly cell-type–specific, differences in the response to low α-T status may have also influenced our findings. For example, cerebellar Purkinje neurons and/or the supportive Bergmann glial cells around them [which express α-TTP (38)] may be more sensitive to α-T status and oxidative stress than other cells. Isolating and analyzing specific cell types could address these questions.

4-HNE concentrations may be a more representative marker of oxidative stress in the cerebellum than the spinal cord. 4-HNE is generated from the oxidation of lipids containing polyunsaturated omega-6 acyl groups, such as linoleic (18:2n–6) or arachidonic (20:4n−6) acids; these fatty acids are typically higher in the rodent brain than the spinal cord (39). Evaluating other markers, such as 3-NT, hydroxyoctadecadienoic acids (t-HODEs), and F2-isoprostanes (7, 10, 40), may give more insight for the spinal cord.

We hypothesized that increased oxidative stress in the cerebellum and spinal cord would result in changes to the myelin-related transcriptome and myelin morphology. Our previous study showed that the HSYN diet, compared with the NAT diet, significantly downregulated myelin genes in cerebella of adolescent (7 wk old) *Ttpa*$^{-/-}$ mice (25). Other work using *Ttpa*$^{-/-}$ mice has demonstrated brain myelin–related gene expression changes at 3 and 10 mo of age (30, 31), spinal cord axon degeneration at 6 mo of age (9), and myelin pathologies as early as 12 mo of age (9) (Figure 5).

Surprisingly, myelin-related genes were not modulated in the current study. We selected genes based on previous *Ttpa*$^{-/-}$ mouse trials, such as transcription factors (*Sox10*, *Myrf*, *Nr1h3*, *Rora*) and genes encoding myelin proteins (e.g., *Mbp*, *Plp1*) (Table 1). Inherent differences in myelination status during adolescence versus adulthood may help explain the discrepancies between studies. During adolescence, the initial myelination phase is fully underway, so myelin-related genes may be naturally upregulated. However, during adulthood, the myelin is established and only slowly being repaired, so dietary impact on myelin-related gene expression may not be detectable.

Consistent with the gene expression results, myelinated axon areas (white matter tracings) were unchanged in *Ttpa*$^{-/-}$ mice. However, we used a gross histological indicator of myelination, so this does not rule out the possibility of microstructural myelin differences. These could be revealed through techniques like transmission electron microscopy (9).

We confirmed (9) that *Necab1*, a calcium-binding protein, is consistently downregulated (~0.2-fold change) in cerebella of *Ttpa*$^{-/-}$ mice, regardless of brain α-T status. These *Necab1* results corroborate previous reports showing that *Ttpa*$^{-/-}$ mice have dysregulated expression of genes encoding calcium channels (32) and calcium signal transducing proteins (30) in neural tissues (dorsal root ganglia and cerebral cortex, respectively). These transcriptomic changes throughout the nervous system could cause diverse and detrimental downstream consequences related to cellular signaling, synaptic function, and energy metabolism,

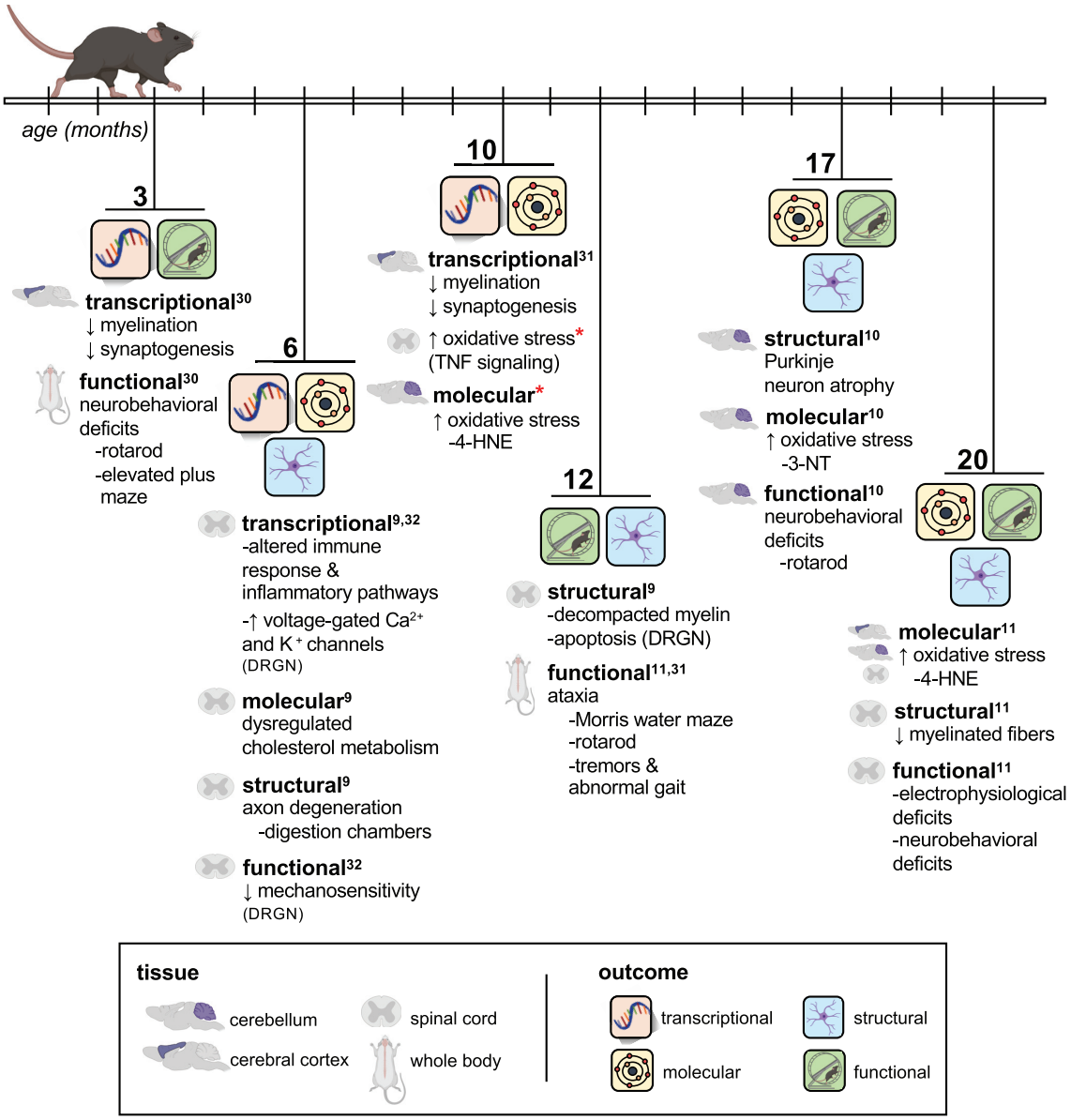

FIGURE 5 Developmental timeline of the neurological phenotype in *Ttpa*$^{-/-}$ mice. Outcomes were reported for mice fed low- or vitamin E–deficient diets. Spinal cord pathologies may develop before other neurological tissues. Transcriptional and molecular outcomes tend to precede structural and functional outcomes. Superscripts reference the studies in which the outcomes were reported. Asterisks (∗) indicate contributions from the current study. DRGN, dorsal root ganglion neurons; *Ttpa*, α-tocopherol transfer protein; 3-NT, 3-nitrotyrosine; 4-HNE, 4-hydroxynonenal.

culminating in neurodegenerative pathologies (41). Disrupted calcium homeostasis may therefore be a key feature and/or cause of the neurological phenotype in *Ttpa*$^{-/-}$ mice.

Conclusions from our study were limited by a few critical factors. One factor was the age of the mice at study termination. We intentionally selected endpoints that were assessed in older mice in order to replicate prior findings and provide new data during an intermediary stage of adulthood. However, 10 mo of age may be premature for detecting deficits, particularly related to the cerebellar Purkinje neurons. Nevertheless, our results provide further insight into the developmental timeline of α-T deficiency–associated pathologies (Figure 5). The relatively mild biochemical changes in response to low α-T status were surprising in this study, since altered oxidative stress and gene expression have been shown at even earlier ages in this mouse model (25, 30, 40).

A second limiting factor was insufficient power in experimental group sizes, which precluded conclusive inferences for some measurement outcomes (e.g., 4-HNE in the cerebellum). This was due to higher than anticipated intragroup variation, particularly the VED diet group.

Last, the choice of fat source for our experimental diets may have influenced our study outcomes. This is because our experimental diets had very low PUFA concentrations compared with other *Ttpa*$^{-/-}$ mouse studies. We replaced the majority of soybean oil (∼60% PUFA), which is standard in rodent diets, with hydrogenated coconut oil (∼2% PUFA) to minimize the vitamin E content. Interestingly, *Ttpa*$^{-/-}$ mice fed high omega-6 PUFA diets (linoleic acid from corn oil) have been reported to display ataxia and other α-T deficiency symptoms at ∼6 mo of age, which was significantly earlier than mice not supplemented with omega-6 PUFAs (42). α-T is well established as a PUFA-protector due to its antioxidant capacity. Furthermore, it is generally accepted that consuming high-PUFA diets also requires higher α-T intakes to meet daily α-T requirements (43–45). Taken together, our low-PUFA diets may have attenuated the pathological progression and the anticipated molecular changes in our VED-fed *Ttpa*$^{-/-}$ mice.

Notably, methodological differences may also partially explain why the current study results do not corroborate our previous study using adolescent mice. In the previous study, female *Ttpa*$^{+/-}$ breeders received a standard AIN-93G diet containing α-T during the initial gestation period (days 1–9) followed by a VED diet for the remainder of gestation and lactation (25, 28). In contrast, breeders for the current adult study received a low-vitamin-E diet for the entire breeding period (28). Both breeder diet strategies successfully minimized the transfer of α-T to offspring; 3-wk-old *Ttpa*$^{-/-}$ weanlings had very low brain α-T concentrations regardless of the breeder diet strategy. Therefore, we assumed that the offspring were also similar in other ways, such as overall α-T and brain development status. However, the maternal diets may have differentially affected study mice before weaning and led to differences for our final outcomes.

We measured α-T stereoisomer profiles in pooled composite brain samples for both the current adult mouse study and our previous adolescent mouse study (25). α-T stereoisomer proportions were similar in both studies. Specifically, *2R* stereoisomers constituted the majority of α-T in *Ttpa*$^{+/+}$ mice fed the CON diet and *Ttpa*$^{-/-}$ mice fed the NAT diet, whereas *Ttpa*$^{-/-}$ mice fed either the SYN or HSYN diets did not discriminate between *2R* and *2S* stereoisomers. It is clear that brain stereoisomer composition is highly dependent on the presence of α-TTP, be it hepatic α-TTP or possibly local brain expression of α-TTP.

We aimed to test the effectiveness of natural versus synthetic α-T for preventing unfavorable neurological outcomes in adult mice. Both α-T sources benefited the neuroinflammatory markers that were elevated in *Ttpa*$^{-/-}$ mice fed the VED diet. However, the effectiveness of natural versus synthetic α-T could not be determined for morphological endpoints since these were unchanged in VED-fed *Ttpa*$^{-/-}$ mice.

Future work should compare the biochemical, histological, and neurobehavioral effects of natural versus synthetic α-T in aging adult *Ttpa*$^{-/-}$ mice (∼17+ mo, when they have more pronounced symptoms of deficiency). These studies should further explore the relative biopotencies of natural and synthetic α-T in neural tissues. The optimal time point for α-T administration is also unknown. Animals in our and others' studies were fed experimental diets from weaning age until being killed. Studies should also test whether short-term α-T-feeding interventions during late adulthood rescue the neurological phenotype.

Despite mostly null findings, our novel *Ttpa*-null mouse study lays the groundwork for future research in this area. Importantly, we have also highlighted potential limitations of using the *Ttpa*$^{-/-}$ mouse model and recommended additional experiments that will help answer our lingering questions.

α-T acts as a neuroprotectant during aging, possibly because it can modulate immune and inflammatory responses. In *Ttpa*$^{-/-}$ mice, neuroinflammation may occur during midlife and cause abnormal neural function and myelination later on. Our study provides a snapshot of the 10-mo-old *Ttpa*$^{-/-}$ mouse cerebellum and spinal cord after 37 wk fed VED or α-T–supplemented diets. Low α-T status causes time- and tissue-dependent abnormalities, but the exact timeline of these consequences has not been determined.

Acknowledgments

The authors acknowledge Drs. Richard Bruno and Sisi Cao at Ohio State University for technical assistance with the α-T stereoisomer analysis. The authors' responsibilities were as follows—KMR, MJK, and JWE: designed the research; KMR and JWE: wrote the manuscript; KMR: conducted the research and analyzed the data; JMJ: provided essential assistance with data interpretation; KMR, MJK, JMJ, and JWE: contributed to manuscript revisions; JWE: had primary responsibility for the final content; and all authors: read and approved the final manuscript.

References

1. Shichiri M. The role of lipid peroxidation in neurological disorders. J Clin Biochem Nutr 2014;54:151–60.
2. Atkinson J, Harroun T, Wassall SR, Stillwell W, Katsaras J. The location and behavior of alpha-tocopherol in membranes. Mol Nutr Food Res 2010;54:641–51.
3. Lemaire-Ewing S, Desrumaux C, Neel D, Lagrost L. Vitamin E transport, membrane incorporation and cell metabolism: is alpha-tocopherol in lipid rafts an oar in the lifeboat? Mol Nutr Food Res 2010;54:631–40.
4. Ulatowski LM, Manor D. Vitamin E and neurodegeneration. Neurobiol Dis 2015;84:78–83.
5. Muller DP. Vitamin E and neurological function. Mol Nutr Food Res 2010;54:710–8.
6. Traber MG, Sokol RJ, Burton GW, Ingold KU, Papas AM, Huffaker JE, Kayden HJ. Impaired ability of patients with familial isolated vitamin E deficiency to incorporate alpha-tocopherol into lipoproteins secreted by the liver. J Clin Invest 1990;85:397–407.
7. Terasawa Y, Ladha Z, Leonard SW, Morrow JD, Newland D, Sanan D, Packer L, Traber MG, Farese RV, Jr. Increased atherosclerosis in hyperlipidemic mice deficient in alpha -tocopherol transfer protein and vitamin E. Proc Natl Acad Sci 2000;97:13830–4.
8. Cavalier L, Ouahchi K, Kayden HJ, Di Donato S, Reutenauer L, Mandel JL, Koenig M. Ataxia with isolated vitamin E deficiency: heterogeneity of mutations and phenotypic variability in a large number of families. Am J Hum Genet 1998;62:301–10.
9. Finno CJ, Bordbari MH, Gianino G, Ming-Whitfield B, Burns E, Merkel J, Britton M, Durbin-Johnson B, Sloma EA, McMackin M, et al. An innate immune response and altered nuclear receptor activation defines the spinal cord transcriptome during alpha-tocopherol deficiency in Ttpa-null mice. Free Radic Biol Med 2018;120:289–302.
10. Ulatowski L, Parker R, Warrier G, Sultana R, Butterfield DA, Manor D. Vitamin E is essential for Purkinje neuron integrity. Neuroscience 2014;260:120–9.
11. Yokota T, Igarashi K, Uchihara T, Jishage K, Tomita H, Inaba A, Li Y, Arita M, Suzuki H, Mizusawa H, et al. Delayed-onset ataxia in mice lacking alpha-tocopherol transfer protein: model for neuronal

degeneration caused by chronic oxidative stress. Proc Natl Acad Sci 2001;98: 15185–90.
12. Yokota T, Uchihara T, Kumagai J, Shiojiri T, Pang JJ, Arita M, Arai H, Hayashi M, Kiyosawa M, Okeda R, et al. Postmortem study of ataxia with retinitis pigmentosa by mutation of the alpha-tocopherol transfer protein gene. J Neurol Neurosurg Psychiatry 2000;68:521–5.
13. Altman J. Postnatal development of the cerebellar cortex in the rat. II. Phases in the maturation of Purkinje cells and of the molecular layer. J Comp Neurol 1972;145:399–463.
14. Optican LM. Low rates yield big returns. Nat Neurosci 1998;1:8–9.
15. Meffre D, Shackleford G, Hichor M, Gorgievski V, Tzavara ET, Trousson A, Ghoumari AM, Deboux C, Nait Oumesmar B, Liere P, et al. Liver X receptors alpha and beta promote myelination and remyelination in the cerebellum. Proc Natl Acad Sci U S A 2015;112:7587–92.
16. Aparicio JM, Belanger-Quintana A, Suarez L, Mayo D, Benitez J, Diaz M, Escobar H. Ataxia with isolated vitamin E deficiency: case report and review of the literature. J Pediatr Gastroenterol Nutr 2001;33:206–10.
17. Gabsi S, Gouider-Khouja N, Belal S, Fki M, Kefi M, Turki I, Ben Hamida M, Kayden H, Mebazaa R, Hentati F. Effect of vitamin E supplementation in patients with ataxia with vitamin E deficiency. Eur J Neurol 2001;8: 477–81.
18. Doria-Lamba L, De Grandis E, Cristiani E, Fiocchi I, Montaldi L, Grosso P, Gellera C. Efficacious vitamin E treatment in a child with ataxia with isolated vitamin E deficiency. Eur J Pediatr 2006;165:494–5.
19. Traber MG, Burton GW, Ingold KU, Kayden HJ. RRR- and SRR-alpha-tocopherols are secreted without discrimination in human chylomicrons, but RRR-alpha-tocopherol is preferentially secreted in very low density lipoproteins. J Lipid Res 1990;31:675–85.
20. Kuchan MJ, Ranard KM, Dey P, Jeon S, Sasaki GY, Schimpf KJ, Bruno RS, Neuringer M, Erdman JW. Infant rhesus macaque brain alpha-tocopherol stereoisomer profile is differentially impacted by the source of alpha-tocopherol in infant formula. J Nutr 2020;150:2305–13.
21. Kuchan MJ, Jensen SK, Johnson EJ, Lieblein-Boff JC. The naturally occurring alpha-tocopherol stereoisomer RRR-alpha-tocopherol is predominant in the human infant brain. Br J Nutr 2016;116:126–31.
22. Rhodes JS, Rendeiro C, Mun JG, Du K, Thaman P, Snyder A, Pinardo H, Drnevich J, Chandrasekaran S, Lai C-S, et al. Brain alpha-tocopherol concentration and stereoisomer profile alter hippocampal gene expression in weanling mice. J Nutr 2020;150:3075–85.
23. Weiser H, Vecchi M. Stereoisomers of alpha-tocopheryl acetate. II. Biopotencies of all eight stereoisomers, individually or in mixtures, as determined by rat resorption-gestation tests. Int J Vitam Nutr Res 1982;52:351–70.
24. Hoppe PP, Krennrich G. Bioavailability and potency of natural-source and all-racemic alpha-tocopherol in the human: a dispute. Eur J Nutr 2000;39:183–93.
25. Ranard KM, Kuchan MJ, Bruno RS, Juraska JM, Erdman JW. Synthetic alpha-tocopherol, compared with natural alpha-tocopherol, downregulates myelin genes in cerebella of adolescent Ttpa-null mice. J Nutr 2020;150:1031–40.
26. Han SN, Pang E, Zingg JM, Meydani SN, Meydani M, Azzi A. Differential effects of natural and synthetic vitamin E on gene transcription in murine T lymphocytes. Arch Biochem Biophys 2010;495:49–55.
27. Burton GW, Traber MG, Acuff RV, Walters DN, Kayden H, Hughes L, Ingold KU. Human plasma and tissue alpha-tocopherol concentrations in response to supplementation with deuterated natural and synthetic vitamin E. Am J Clin Nutr 1998;67:669–84.
28. Ranard KM, Kuchan MJ, Erdman JW, Jr. Breeder diet strategies for generating Ttpa-null and wild-type mice with low vitamin E status to assess neurological outcomes. Curr Dev Nutr 2020;4:nzaa155.
29. Jeon S, Neuringer M, Kuchan MJ, Erdman JW, Jr. Relationships of carotenoid-related gene expression and serum cholesterol and lipoprotein levels to retina and brain lutein deposition in infant rhesus macaques following 6 months of breastfeeding or formula feeding. Arch Biochem Biophys 2018;654:97–104.
30. Gohil K, Schock BC, Chakraborty AA, Terasawa Y, Raber J, Farese RV, Jr, Packer L, Cross CE, Traber MG. Gene expression profile of oxidant stress and neurodegeneration in transgenic mice deficient in alpha-tocopherol transfer protein. Free Radic Biol Med 2003;35:1343–54.
31. Gohil K, Godzdanker R, O'Roark E, Schock BC, Kaini RR, Packer L, Cross CE, Traber MG. Alpha-tocopherol transfer protein deficiency in mice causes multi-organ deregulation of gene networks and behavioral deficits with age. Ann N Y Acad Sci 2004;1031:109–26.
32. Finno CJ, Peterson J, Kang M, Park S, Bordbari MH, Durbin-Johnson B, Settles M, Perez-Flores MC, Lee JH, Yamoah EN. Single-cell RNA-seq reveals profound alterations in mechanosensitive dorsal root ganglion neurons with vitamin E deficiency. iScience 2019;21:720–35.
33. Schindelin J, Arganda-Carreras I, Frise E, Kaynig V, Longair M, Pietzsch T, Preibisch S, Rueden C, Saalfeld S, Schmid B, et al. Fiji: an open-source platform for biological-image analysis. Nat Methods 2012;9:676–82.
34. Hoxha E, Gabriele RMC, Balbo I, Ravera F, Masante L, Zambelli V, Albergo C, Mitro N, Caruso D, Di Gregorio E, et al. Motor deficits and cerebellar atrophy in Elovl5 knock out mice. Front Cell Neurosci 2017;11:343.
35. Devaraj S, Jialal I. Alpha-tocopherol decreases tumor necrosis factor-alpha mRNA and protein from activated human monocytes by inhibition of 5-lipoxygenase. Free Radic Biol Med 2005;38:1212–20.
36. Li CJ, Li RW, Kahl S, Elsasser TH. Alpha-tocopherol alters transcription activities that modulates tumor necrosis factor alpha (TNF-alpha) induced inflammatory response in bovine cells. Gene Regul Syst Bio 2012;6: 1–14.
37. Han SN, Wu D, Ha WK, Beharka A, Smith DE, Bender BS, Meydani SN. Vitamin E supplementation increases T helper 1 cytokine production in old mice infected with influenza virus. Immunology 2000;100:487–93.
38. Hosomi A, Goto K, Kondo H, Iwatsubo T, Yokota T, Ogawa M, Arita M, Aoki J, Arai H, Inoue K. Localization of alpha-tocopherol transfer protein in rat brain. Neurosci Lett 1998;256:159–62.
39. Salem NM, Lin YH, Moriguchi T, Lim SY, Salem N, Jr., Hibbeln JR. Distribution of omega-6 and omega-3 polyunsaturated fatty acids in the whole rat body and 25 compartments. Prostaglandins Leukotrienes Essent Fatty Acids 2015;100:13–20.
40. Yoshida Y, Itoh N, Hayakawa M, Habuchi Y, Saito Y, Tsukamoto Y, Cynshi O, Jishage K, Arai H, Niki E. The role of alpha-tocopherol in motor hypofunction with aging in alpha-tocopherol transfer protein knockout mice as assessed by oxidative stress biomarkers. J Nutr Biochem 2010;21: 66–76.
41. Zundorf G, Reiser G. Calcium dysregulation and homeostasis of neural calcium in the molecular mechanisms of neurodegenerative diseases provide multiple targets for neuroprotection. Antioxid Redox Signaling 2011;14:1275–88.
42. Ulatowski L, Thakur V, Manor D, Parker R. Vitamin E protects against PUFA-induced behavioral and motor deficits. FASEB J 2014;28(Suppl 596.8).
43. Raederstorff D, Wyss A, Calder PC, Weber P, Eggersdorfer M. Vitamin E function and requirements in relation to PUFA. Br J Nutr 2015;114: 1113–22.
44. Valk EE, Hornstra G. Relationship between vitamin E requirement and polyunsaturated fatty acid intake in man: a review. Int J Vitam Nutr Res 2000;70:31–42.
45. Horwitt MK. Vitamin E and lipid metabolism in man. Am J Clin Nutr 1960;8:451–61.